SAJSET
ISSN: 2992-3581

*Savannah Journal of Science and Engineering Technology*
*Volume: 03; Issue: 06; Pages: 638-646; 2025.*
www.sajsetjournal.com.ng

*DOI: xx.xxxx.x/sajset-03-2025-0088*

SAJSET
ISSN: 2992-3581

# Characterisation of PLA-based biocomposites reinforced with sugarcane bagasse and paper fibre

[1]Abdulmalik, S. S., [1]Muhammad, J. Y. and Bala, A.
*[1]Department of Mechanical Engineering, Nigerian Army University Biu, P.M.B. 1500, Borno State, Nigeria*
muhdjy87@gmail.com, anasbala24@gmail.com

***Paper History***
*Received: 01st Nov., 2025*
*Accepted: 24th Nov., 2025*
*Published: November, 2025*

***Abstract:***
*The widespread issue of plastic pollution necessitates the development of sustainable, high-performance biocomposites. This study developed fully biodegradable PLA-based biocomposites reinforced with sugarcane bagasse (SB) and paper fibres to reduce cost and environmental impact. Composites containing up to 30 % filler were produced using two-roll milling and compression molding. FTIR analysis confirmed successful incorporation of lignocellulosic fillers and indicated hydrogen bonding between PLA carbonyl and filler hydroxyl groups, suggesting good interfacial interaction. Mechanical tests showed that hardness increased with filler content, reaching 42 HV at 30%, while tensile strength peaked at 26 MPa for 25% filler, then declined due to fibre clustering seen in SEM. The composites became more hydrophilic with increasing fibre content. Overall, the 25% filler composite achieved the best balance of strength and hardness, demonstrating a sustainable and cost-effective method for upcycling agricultural and paper waste into high-performance PLA biocomposites. These findings show the potential of PLA-sugarcane bagasse-paper fibre composites as biodegradable alternative for single-use plastics in packaging and food plates.*

*Corresponding author*
*Abdulmalik, S. S.*
alhajisani.sa@gmail.com

***Keywords:*** *Biocomposites, PLA, Paper fibre, Sugarcane bagasse, Sustainable materials*

## 1. Introduction

Plastics and environmental pollution poses serious problems to today's society. The development of composite polymers with high added value is a crucial task since, although certain polymer waste processing methods have been established [1], several of them are still unprofitable. Consequently, the development of biocomposite is important in order to mitigate the environmental impact of plastic products. This effort has received priority

Among these biodegradable polymers, polylactic acid (PLA) is produced and used in the largest quantities [2] and thus plays a leading role in the sustainable plastic economy [3]. Being derived naturally from agricultural products, such as corn and wheat [4], PLA is biodegradable and has numerous excellent Physico-mechanical characteristics, including outstanding melt processing ability, high strength, a low thermal expansion coefficient, low elongation at break, and no cracking into large pieces [5]. However, its inherent drawbacks, especially its much higher cost compared with general-purpose plastics such as polyethylene and propylene, have hampered its wider practical application [6].

Natural fibres are inexpensive, have a low specific weight, and have good particular mechanical qualities. They are also widely available in nature. They have the potential to be substitute composite materials due to their quick renewability. A variety of natural fibres, including wood fibre [7], bamboo[8], rice husk and wheat husk [9], and straw fibres (sorghum, rice, corn, and soybean) [10] as well as their hybrids [11], have already been complexed with a number of polymers to accomplish various goals. Cellulose nanocrystals are occasionally used as reinforcement for these polymers [12]. In PLA-based composites, the majority of these natural fibbers have also been used as reinforcements. One of the most significant natural fibres, sugarcane bagasse (SB) is a residue that is produced in large quantities for the sugar industry. It is inexpensive, plentiful (an average of 675 million tons of bagasse are produced annually as waste material [13], and biodegradable. A lot of sugarcane bagasse (SB) is often burned, which causes pollution and wastes a valuable resource, so its use is limited. Reusing SB is therefore very important. One of the most common ways to reuse it is by making composites with a polymer matrix. SB is made up of about 40–50% cellulose, 25–35% hemicellulose, and 25–28% lignin [14]. The high concentration of cellulose, which has a crystalline structure, allows SB to perform optimally as a composite reinforcement [13], and some publications have reported on this topic. Patil, *et al.* [14] studied a compression-molded composite made from sugarcane bagasse (SB) and a hybrid resin (a mix of epoxy and natural resins like dammar, pine, and cashew nutshell liquid). The composite's mechanical strength,

weight loss in soil, microbial breakdown, and $CO_2$ release were all affected by the type of natural resin used and the mixing ratio of SB to epoxy–natural resin. Anggono et al. [15] made a sugarcane bagasse (SB)/polypropylene (PP) composite, using wood fibre (WF) as a reference. They found that SB could reinforce PP just as well as other natural fibres—both SB- and WF-reinforced composites showed similar properties and improved impact resistance compared with pure PP. However, because SB is a water-loving (hydrophilic) fibre and PP is water-repelling (hydrophobic), the fibres did not bond well with the polymer, leading to weaker overall physical and mechanical properties. To fix this problem, Vidyashri et al. [16] chemically treated sugarcane bagasse (SB) using alkaline, permanganate, and phosphoric acid methods, then tested the mechanical properties of composites made with treated and untreated fibres in epoxy. The treatments improved both the Young's modulus and tensile strength, with permanganate treatment giving the best results. Compared with pure epoxy, the Young's modulus increased by 22.8% and the tensile strength by 40.6%. Lalta et al. also found that alkaline treatment could improve the mechanical properties of an SB/epoxy composite. [17]. They also observed that the type and length of the fibre had a strong impact on the composite's properties.

To address the drawbacks of polylactic acid (PLA)—such as its high cost, resource waste, and environmental impact and to make better use of sugarcane bagasse (SB) and paper, this study prepared a fully biodegradable composite made from PLA, SB, and paper fibres. For the first time, the physical, mechanical, and microstructural properties of this composite were systematically studied

## 2. Materials and methods

### 2.1. Materials

Polylactic acids (PLA) as matrix, Sugarcane bagasse (SB), paper as reinforcements were the materials used in this study. The proportions of each material are as shown in Table 1. Plate 1 show the materials used.

### 2.2. Materials Processing

The materials were first milled and mixed on a two-roll mill at 190 °C. Then, the samples were molded, compressed, and cured in a molding machine at 160 °C for 5 minutes under a pressure of 2.5 Pa. Plate 2 depicts the samples prepared.


Plate 1: PLA, SB and paper used for this study

Table 1: Material used and their amounts in the composites

| Designation | PLA (%) | SB (%) | Paper (%) |
|---|---|---|---|
| Sample A | 100 | 0 | 0 |
| Sample B | 90 | 5 | 5 |
| Sample C | 85 | 10 | 5 |
| Sample D | 80 | 15 | 5 |
| Sample E | 75 | 20 | 5 |
| Sample F | 70 | 25 | 5 |


Plate 2: The processed samples of the study

### 2.3. Methods

#### 2.3.1. Fourier transform infrared (FTIR)

Fourier transform infrared (FTIR) Spectroscopy was used to analyse the surface components and the functional groups present in the sample. The FTIR analysis was done at a range of 4000-650 $cm^{-1}$ and resolution of 4 $cm^{-1}$ as per ASTM E1252-98.

#### 2.3.2. Water Absorption

The procedure followed ASTM D647 (2010). Initially, 2 g of each biodegradable plate sample were weighed ($W_0$) before soaking in distilled water. Samples were soaked for 5, 10, 15, 20, 25, and 30 minutes. After each soaking period, the sample was removed, blotted with tissue paper, and weighed ($W_1$). Plate 3 provides the set up for the experiment. The percentage of water uptake ($W_T$) was then calculated using equation 1:

$$W_T \frac{W_1 - W_0}{W_0} \times 100 \quad (1)$$

Where $W_1$ = weight of the sample after immersing in water $W_0$ = initial weight of the sample.

#### 2.3.3. Oil absorption

The procedure and formular that was used above for water absorption was also applied to oil absorption analysis. However, oil was used in place of water for soaking of the samples (ASTM D281-12, (2021)).

#### 2.3.4. Tensile strength measurements

The test was conducted using on a Tensile strength test machine Model: TM2101-T7 with a capacity of 10KN. The standard used for this was ASTM D-638.

#### 2.3.5. Hardness test

Vickers hardness test was performed as per ASTM E-384 standard using digital hardness tester (Model:

MV1-PC) with a capacity of 0.3 kgf. The surfaces of the samples were polished by fine sand papers so that flat and smooth surfaces were obtained for accurate results.

### 2.3.6. Thermogravimetric analysis (TGA)

All samples were prepared with a weight of 5 mg to analyze the thermal stability. The test setup was carried out at 30–500 °C with a heating rate of 10 °C /min under nitrogen conditions.

### 2.3.7. Scanning electron microstructure analysis

The selected samples were analyzed using a Zeiss Sigma300VP (GEMINI 1) Scanning Electron Microscope with embedded SmartEDX detector. The samples were prepared on a 12 mm sample stud sited on an adhesive carbon tape and allowed to dry over a 24-hour period. The sample stud was then fastened to a single sample holder and placed the instrument stage inside the instrument chamber for analysis The High-resolution images were captured to assess the surface structure. The SEM operated with a working distance (WD) of (-) under a high vacuum mode at 25 kv utilizing a SE2 DETECTOR to provide detailed morphological information, which was then transferred to the EdX software (Zeiss smart edx) for analysis.

### 2.3.8. Energy dispersive x-ray spectroscopy (EDX)

For elemental analysis, an Energy Dispersive X-ray Spectroscopy (EDX) detector integrated with the SEM was used. Elemental analysis was carried out using the spot method to determine the compositional information. The SEM-EDX result provided shows an image of the sample showing the spot tested, a peak chart showing the intensity of the elements and a table showing the elements (weight %, MDL value and Atomic %).

## 3. Results and discussions

### 3.1 Water absorption

The water absorption of the samples is presented in Figure 1. It can be seen that increasing the proportion of sugarcane bagasse led to higher water absorption rates. This is attributed to the cellulose fibers' molecular structure, which contains numerous polar hydroxyl groups, making them strongly hydrophilic. These findings are consistent with previous reports in the literature [18].

### 3.2 Oil Absorption

The percentage of oil uptake rose with increasing fibre content compared to pure PLA, as shown in Figure 2. The trend indicates that Sample F exhibited the highest oil absorption, followed by Sample B, while Sample C had the lowest among the biocomposites. Previous studies [19] have reported that oil absorption generally increases with higher reinforcement content and longer soaking times.

### 3.3 Hardness

Figure 3 shows the hardness (HV) of six samples (A–F). From the figure it was observed that Sample A has the lowest hardness (~16 HV), while Sample F has the highest (~42 HV). Hardness increases progressively from Sample A to Sample F. The trend suggests that the material composition or fibre content changes systematically across the samples, resulting in a steady increase in hardness.

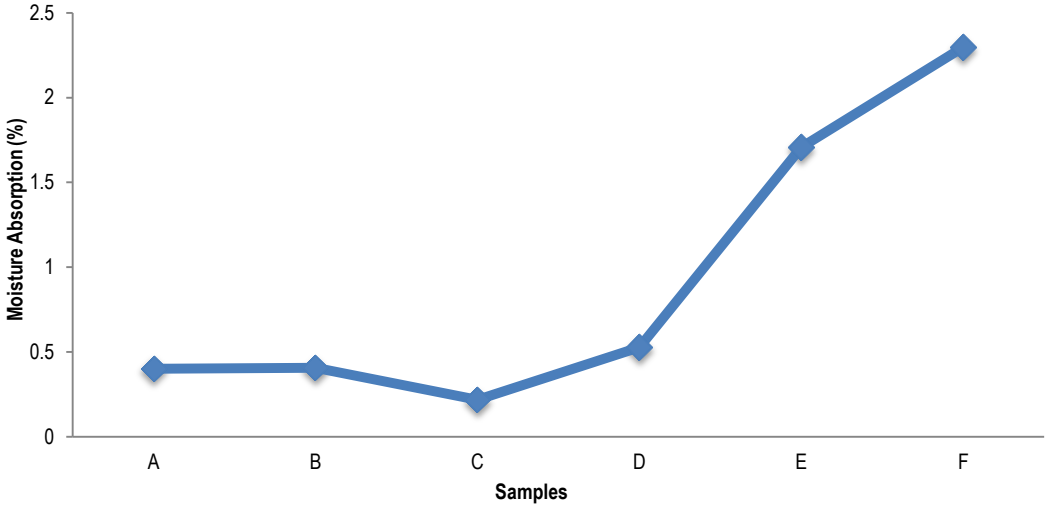


Figure 1: Water absorption of the different samples

This indicates that whatever variable was increased from Sample A to F (e.g., filler content, reinforcement, or processing parameter) directly improved the material's resistance to indentation. The consistent upward trend also suggests a strong correlation between this variable and hardness. Past study showed that hardness increased with increase in filler content [20].

### 3.4 Tensile Strength

Figure 4 illustrates the variation in the tensile strength of six distinct material samples; the tensile strength of six samples, labelled A to F. Tensile strength measures how much pulling force a material can handle before breaking. Sample E has the highest tensile strength at about 26.0 MPa, making it the strongest. Samples A

(≈13.5 MPa) and F (≈14.5 MPa) are the weakest and would break under much less force. Samples B, C, and D have intermediate strengths, ranging from 20.5 MPa (D) to 22.5 MPa (C), with C slightly stronger than B, and B slightly stronger than D. The large difference between the strongest (E) and weakest (A) samples shows significant variation in the material properties This tallies with what was reported in [21].

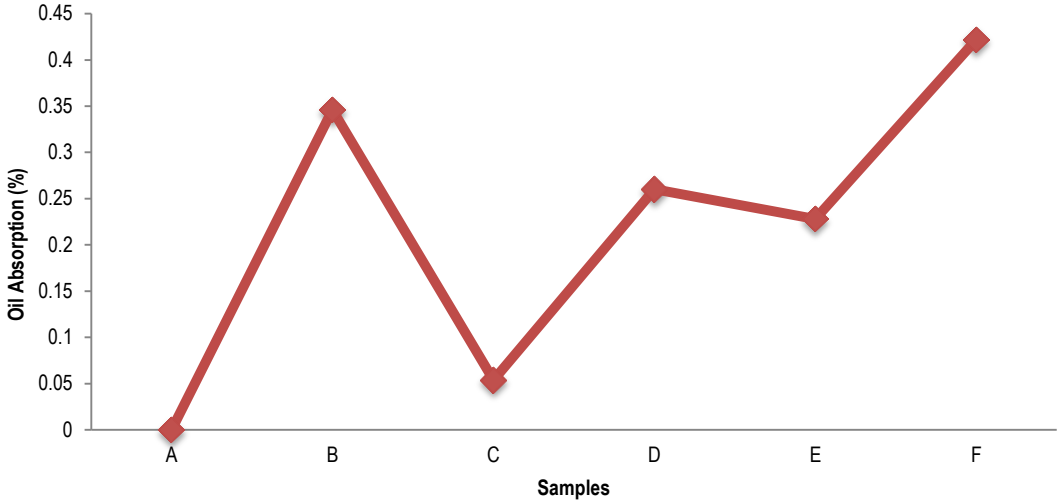


Figure 2: The oil absorption of the samples.

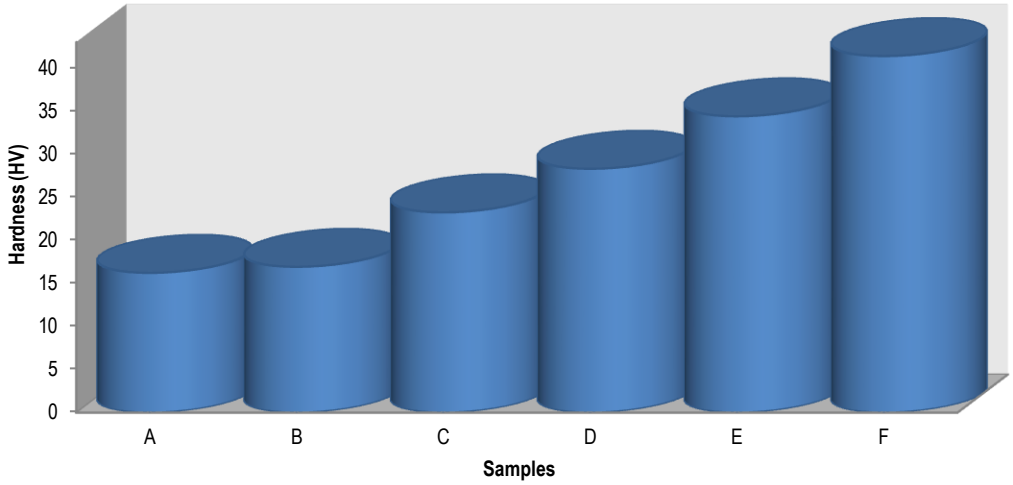


Figure 3: The hardness results of the samples

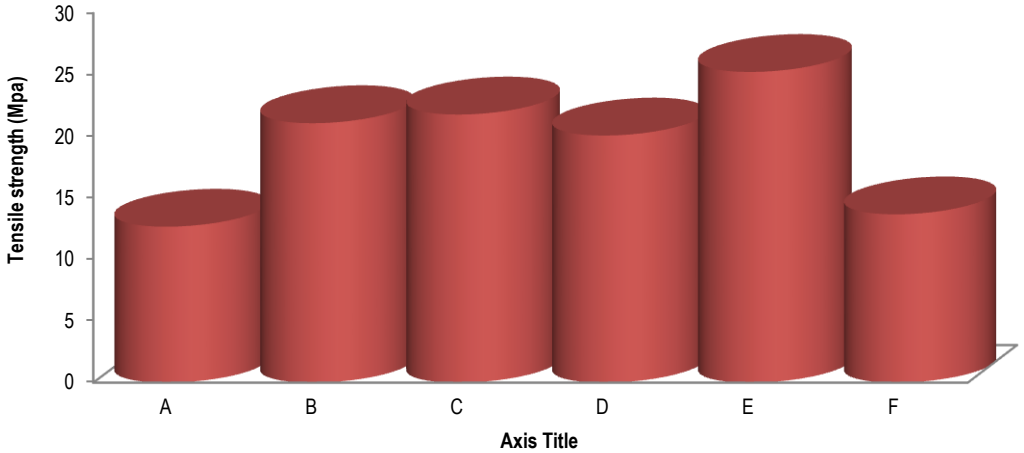


Figure 4: Tensile strength of the samples

## 3.5 FTIR (Fourier-Transform Infrared) spectrum

### 3.5.1 Sample A

Figure 5 provided image is an FTIR (Fourier-Transform Infrared) spectrum of Poly (lactic acid), commonly known as PLA. The spectrum's key features correspond to the characteristic functional groups within the PLA polymer structure. The strongest peak appears around 1745–1760 $cm^{-1}$, showing the carbonyl (C=O) stretching vibration of the ester group in the PLA backbone. This peak is very clear in the image, confirming the presence of the polyester structure. Its exact position can change depending on how crystalline the polymer is. Peaks between 1080–1200 $cm^{-1}$ correspond to the C–O single bond stretching and the asymmetric and symmetric stretching of the C–O–C bonds within the ester group.

### 3.5.2 Sample B

Figure 6 shows the IR spectrum of a composite with 90% PLA, 5% sugarcane bagasse (SB), and 5% paper. The broad O–H band at 3432.9 $cm^{-1}$ indicates hydrogen bonding in the fibres, suggesting some interfacial interaction with PLA. The C=O peak at 1718.3 $cm^{-1}$ is lower than in pure PLA (≈1750 $cm^{-1}$), supporting the presence of hydrogen bonding between PLA carbonyl groups and the fibers' hydroxyl groups.

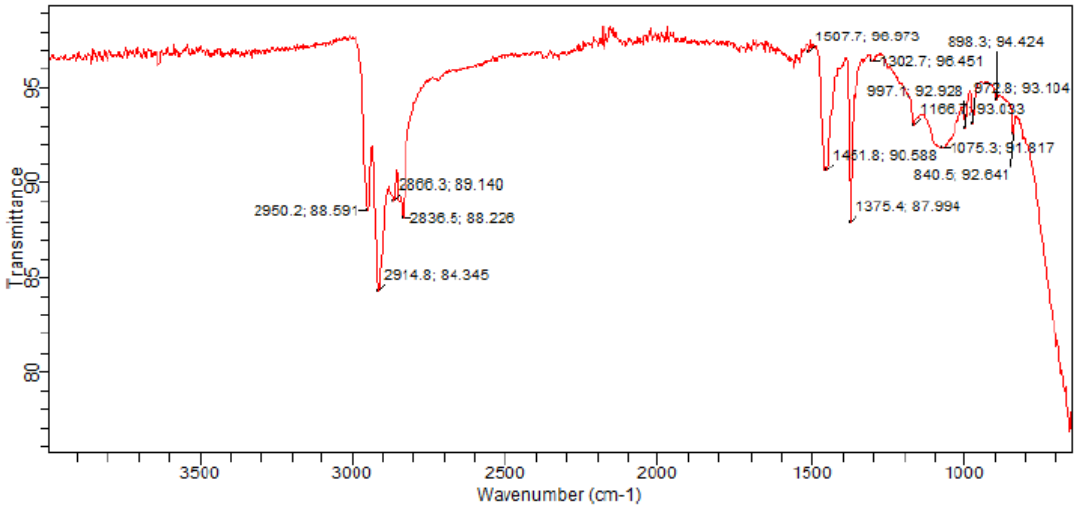


Figure 5: Sample A FTIR spectra.

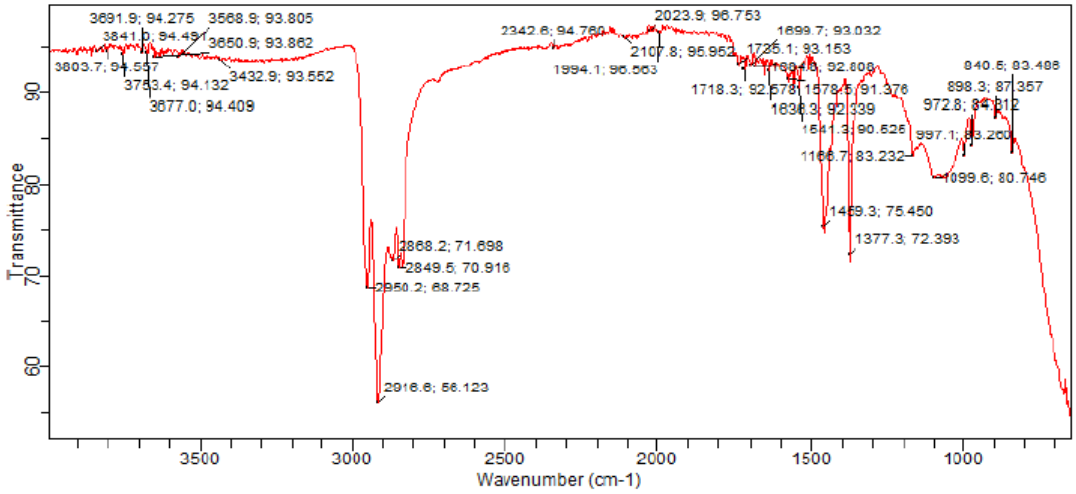


Figure 6: Sample *E* FTIR spectra

### 3.5.3 Sample F

Figure 7 indicates the FTIR spectra of sample F. In essence, the high 30 % filler load is confirmed by the maximal depth of the hydroxyl band at 3400 $cm^{-1}$, which highlights the composite's potential for high moisture uptake, and by the enhanced C-O stretching signals around 1000-1050 $cm^{-1}$.

It also shows that the peak of (C=O) at 1735 – 1718 $cm^{-1}$ providing critical evidence of beneficial hydrogen bonding that aids in stress transfer, while the (C-H) peaks (2915 $cm^{-1}$) serve to confirm the expected mass reduction of the (PLA) component.

## 3.6 Thermogravimetric analysis (TGA)

### 3.6.1 TGA of Sample A

The minimal weight loss below 300 °C shows that the sample is dry, with no substantial water content or significant amounts of volatile low-molecular-weight

residuals (such as leftover lactide or solvents). This demonstrates the PLA polymer's high initial thermal stability (Figure 8). The material starts to break down at around 300 °C, which is important because it sets the maximum safe temperature for processing methods like extrusion or injection molding. The fastest breakdown happens between roughly 350 °C and 450 °C. PLA mainly degrades by breaking its chains into lactide monomers, short chains, and some cyclic molecules. The single, sharp drop in the curve shows that the 100% PLA sample is uniform.

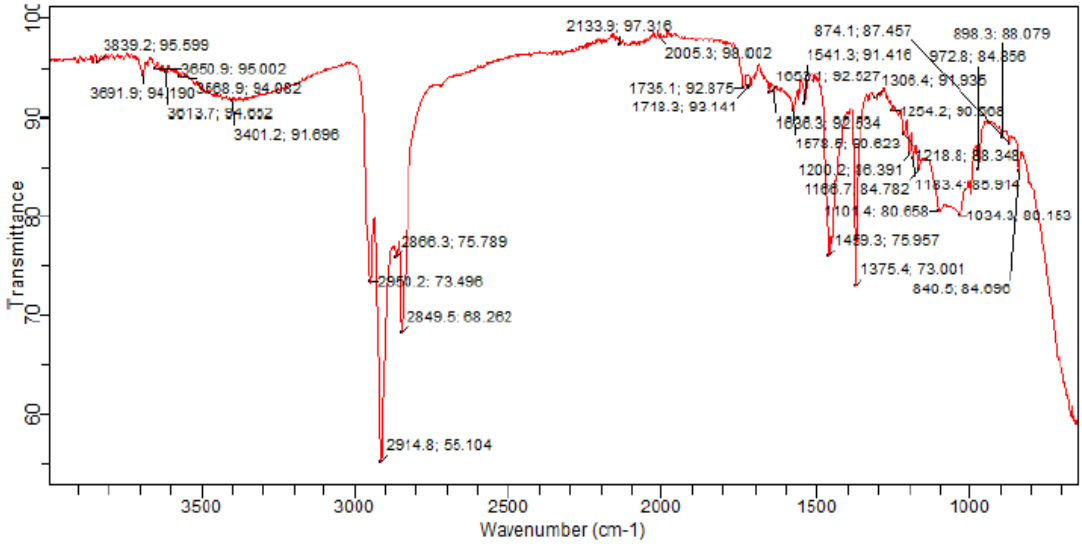


Figure 7: Sample F FTIR spectra

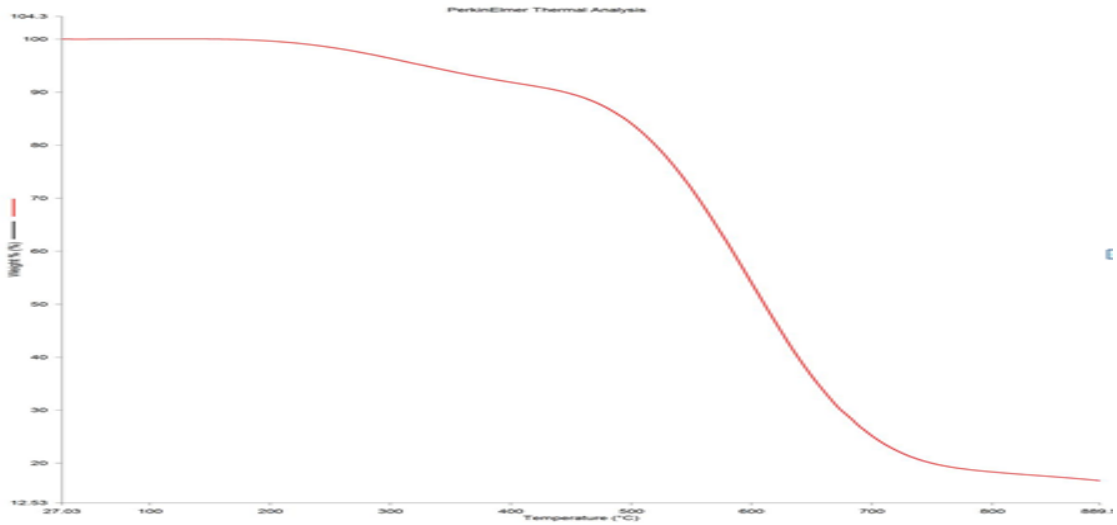

Figure 8: TGA of sample A

### 3.6.2 Thermal stability changes in PLA/SB/paper composites

#### 3.6.2.1 Two-step degradation profile

Natural fibres (sugarcane bagasse and paper) are made of lignocellulose and break down at much lower temperatures than PLA. The composite's TGA curve will show the degradation of both the PLA and the fibres.

First Degradation Step (200 °C to 350 °C): This step mainly shows the breakdown of the hemicellulose and cellulose in the sugarcane bagasse and paper. Hemicellulose, being less stable, degrades first, followed by cellulose.

Second Degradation Step (300 °C to 450 °C): This step represents the main breakdown of the PLA matrix (as seen in pure PLA) and the lignin in the fibres, since lignin is the most heat-resistant part of natural fibres. Changes in Onset Temperature ($T_{onset}$): Adding natural fibres usually lowers the thermal stability of the PLA composite, so it begins to degrade at a lower temperature.

Final Residue at 950 °C: The leftover residue will be much higher than the 12.5% seen for pure PLA. This residue comes from the inorganic part of PLA plus the ash from sugarcane bagasse and paper. The ash in SB and paper usually ranges from 1% to 10%. In a composite with 70% PLA and 30% filler (25% SB + 5% paper), the final residue would equal the 12.5% from the PLA plus the ash from the 30% fibres. This also provides a way to check the actual amount of filler in the composite.

## 3.7 Microstructure of selected samples.

### 3.7.1 SEM of sample B

Figure 9 shows the microstructure of sample B and it reveals two distinct regions: a bright, continuous PLA matrix and darker, irregular filler particles composed of sugarcane bagasse and paper fibres. Several dark circular or elongated areas—particularly in the lower centre and upper right—represent either the filler particles or voids created when these particles were pulled out during fracture. The dark regions (voids or pull-outs) range from less than 1 µm to about 10 µm, consistent with the typical sizes of ground sugarcane bagasse and processed paper fibres. The many dark spots—especially those with smooth, clean internal surfaces—indicate that filler particles were pulled out of the PLA matrix, signifying poor interfacial adhesion. Although clear macro-gaps are not easily visible, the presence of these pull-out voids confirms weak chemical bonding between the hydrophilic natural fibres and the hydrophobic PLA matrix.

### 3.7.2 SEM of Sample F

In Figure 10, the image shows many dark, uneven regions that represent the SB and paper fibres, or more likely, voids and holes left after the fibres were pulled out during breaking. This supports the presence of a high 25 % amount of filler in the material.

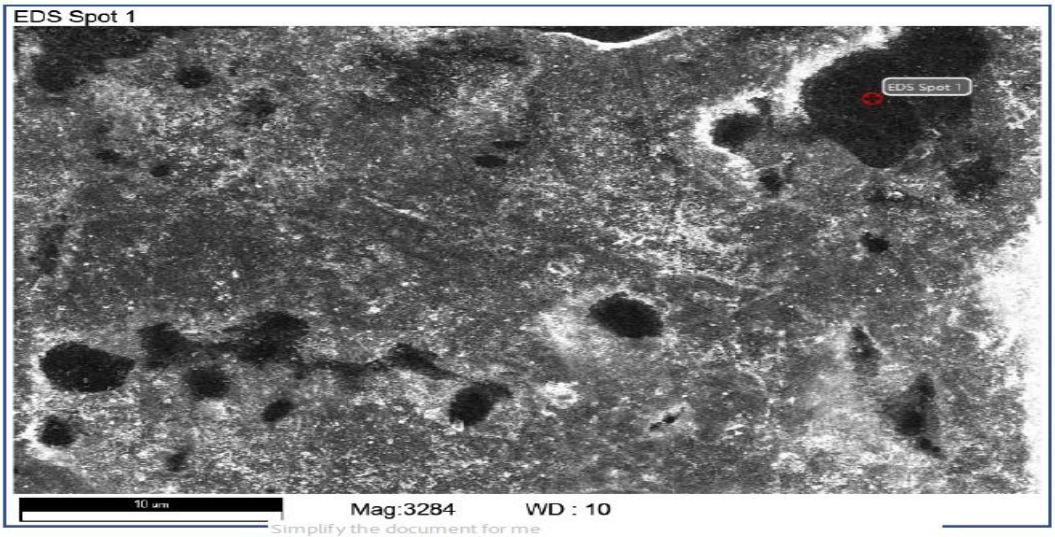


Figure 9: SEM of sample B

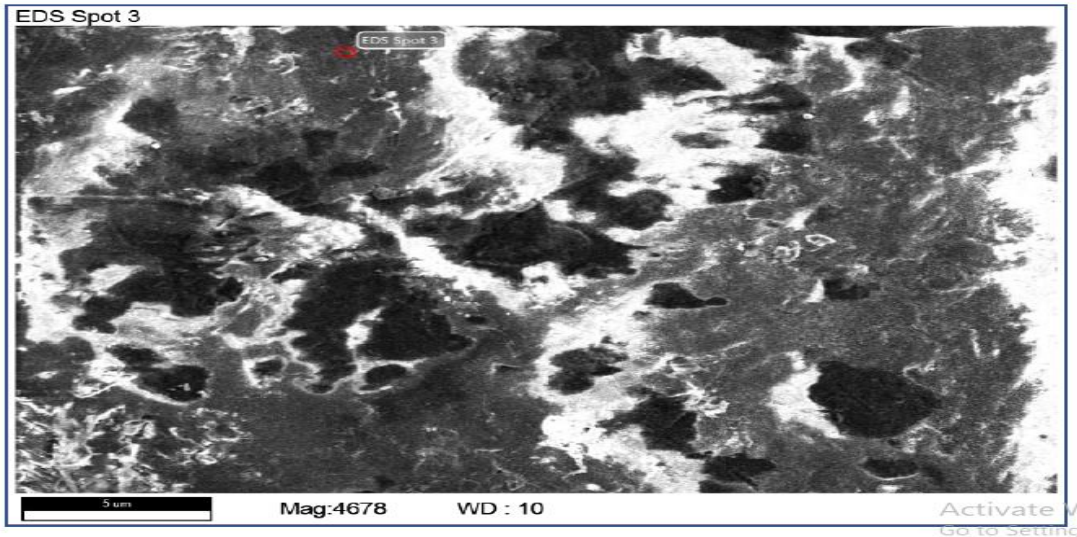


Figure 10: SEM of sample F

Some dark areas appear grouped or connected, showing that the fibres have clumped together. Because there's less PLA matrix (75%) to properly cover and bind the large amount of filler (25%), the fibres touch each other and form clusters. These clusters are weak spots that break easily, showing that the filler is not evenly spread throughout the material. This is as depicted in Figure 10.

### 3.7.3 EDX of Sample B

Figure 11 clearly shows a large amount of carbon and oxygen, confirming the presence of the PLA matrix and the lignocellulosic fillers. The visible peaks for titanium (Ti) show that the commercial PLA matrix includes an inorganic additive, probably TiO. The elements silicon (Si) and calcium (Ca), which come from natural biomass, also

appear—confirming that sugarcane bagasse and paper fillers are part of the material.

### 3.7.4 Sample E

The elemental composition sample E is provided in Figure 12. The biggest peak (marked 'C') shows that the material mainly contains carbon, which makes up its organic structure. The next biggest peak (marked 'O') indicates that the material has a lot of oxygen, coming from the PLA's ester bonds and the many O–H groups in the 30% lignocellulosic filler (SB/Paper). The presence of carbon (C), oxygen (O), and inorganic elements like silicon (Si) and calcium (Ca) confirms that the 30% filler (SB/Paper) was successfully mixed into the PLA material.

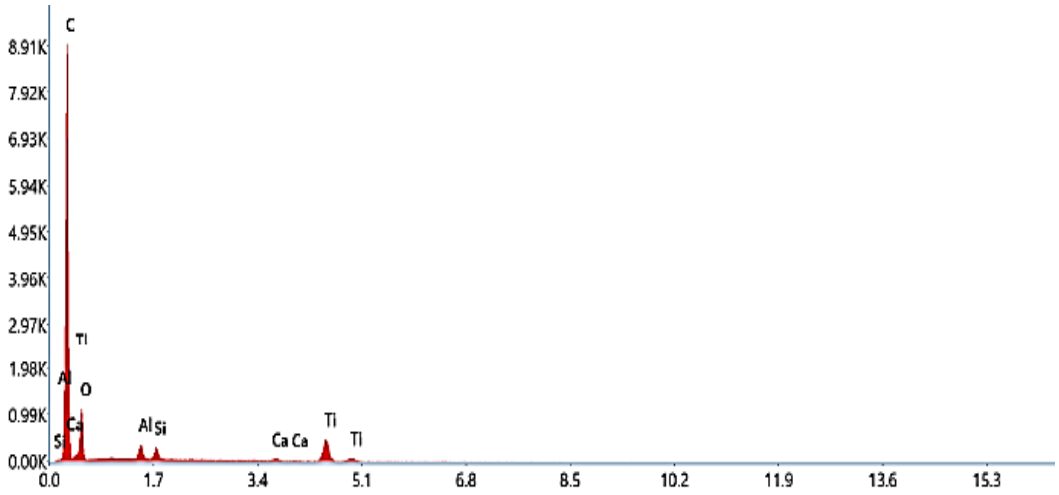


Figure 11: The EDX spectrum for sample B.

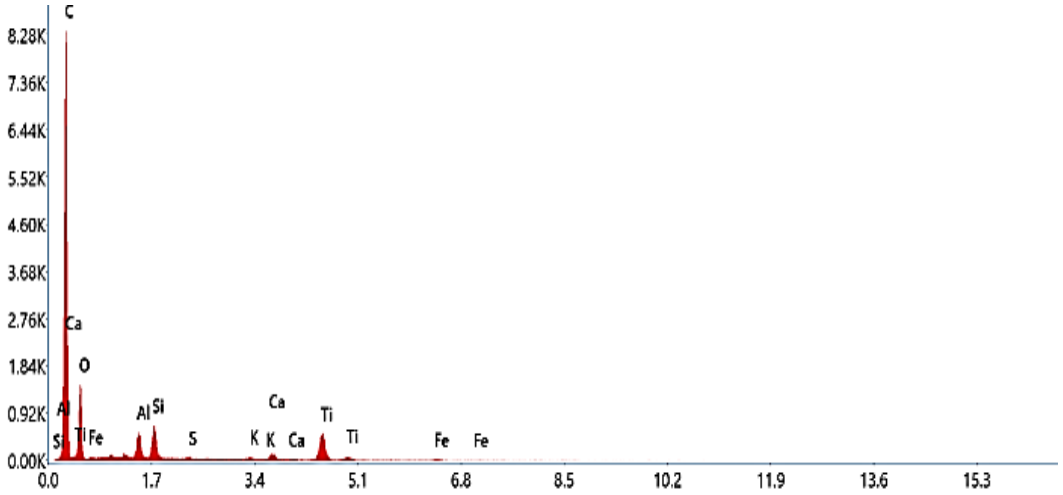


Figure 12: The EDX spectrum for sample E

The EDX analysis confirms that the sample E composite contains an organic base material mixed with a complex set of minerals that come from the PLA additives and the large amount of sugarcane bagasse and paper ash.

## 4. Conclusion

This study focused on creating fully biodegradable polymer composites using Polylactic Acid PLA reinforced with sustainable waste materials: sugarcane bagasse (SB) and paper fibres. FTIR analysis confirmed the successful incorporation of the fillers and, most importantly, provided strong evidence of favourable hydrogen bonding between the filler's hydroxyl (OH) groups and the PLA}'s carbonyl (C=O) groups (indicated by a C=O peak shift to approximately 1718 $cm^{-1}$. Hardness significantly increased with fibre content, peaking at 42 HV for the highest load (Sample F, 30 % filler). Tensile Strength was optimized at an intermediate load ~ 26.0MPa for Sample E), with excessively high loads (Sample F) causing a reduction due to fibre clustering. The high concentration of OH groups in high-load samples led to increased water absorption, confirming the hydrophilic nature of the composites. TGA analysis showed a reduction in thermal stability compared to pure PLA due to the earlier degradation of the lignocellulosic components. SEM analysis revealed poor interfacial adhesion (fibre pull-out) in low-load samples and fibre clustering in high-load samples, which explains the drop in tensile strength at 30 % filler content. EDX confirmed the successful mixing of all components. This result paves way for further study to developed alternative biodegradable food plate.

## Acknowledgement

The authors wish to acknowledged NAUB directorate for research and innovation, for the award of TETFUND institution based research project 2024

## References

[1]. Ma, Y., (2018). Changing Tetra Pak: From waste to resource, *Science Progress*, 101, (2), 161–170.

[2]. Józó, M., Várdai, R., Bartos, A., Móczó, J. and Pukánszky, B., (2022). Preparation of Biocomposites with Natural Reinforcements: The Effect of Native Starch and Sugarcane Bagasse Fibers, *Molecules*, 27(19), 6423

[3]. Szatkowski, P., Gralewski, J., Suchorowiec, K., Kosowska, K., Mielan, B. and Kisilewicz, M., (2024). Aging Process of Biocomposites with the PLA Matrix Modified with Different Types of Cellulose, *Materials (Basel).*, 17(1), 1–18.

[4]. Carlos Ramirez, V. P. and Agaliotis, E., (2024). Fracture toughness and overall characterization of PLA based biocomposites with natural fibers: A comparative study, *Polymer (Guildf).*,307, 127309.

[5]. Azka, S. M. S., Adlan, M., Zainudin, H. A. E. S. and Aziz, F. A., (2024). An examination of recent research of water absorption behavior of natural fiber reinforced polylactic acid (PLA) composites: A review, *International Journal of Biological Macromolecules*, 268(1), 131845.

[6]. Huo, X., Wan, P., Zhang, R., Zhang, Z. and Shanshan, L. V., (2024). Enhancing the strength and toughness of polylactic acid-based composites through one-step co-deposition of active coating onto wood fiber, *International Journal of Biological Macromolecukes*, 274,1, 133414.

[7]. Paczkowski, P., Puszka, A., Miazga-Karska, M., Ginalska, G. and Gawdzik, B., (2021). Synthrsis , Characterization and Testing of Antimicrobial Activity of Composites of Unsaturated Polyester Resins with Wood Flour and Silver Nanoparticles, *Materials (Basel)*, 14,05, 1122.

[8]. Gao, J., Zhang, Y. Bi, Y., Du, K., Su, J. and Zhang, S., (2024). A strong hydrogen bond bridging interface based on tannic acid for improving the performance of high-filled bamboo fibers/poly (butylene succinate-co-butylene adipate) (PBSA) biocomposites, *International Journal of Biological Macromolecules*, 267, 2, 131611.

[9]. Muthuraj, R., Lacoste, C., Lacroix, P. and Bergeret, A., (2019). Sustainable thermal insulation biocomposites from rice husk, wheat husk, wood fibers and textile waste fibers: Elaboration and performances evaluation, *Industrial Crops and Products*, 135, 238–245.

[10]. Feng, J., Zhang, W., Wang, L. and He, C., (2020). Performance comparison of four kinds of straw/PLA/PBAT wood plastic composites, *BioResources*, 15(2), 2596–2604.

[11]. Sriseubsai, W. and Praemettha, A., (2025). Hybrid natural fiber composites of polylactic acid reinforced with sisal and coir fibers, *Polymers (Basel).*, 17(1), 1-64.

[12]. Handan, P., Mahmoud, A., Tamer, U. and Kayaoglu, B. K., (2025). Cellulose nanocrystal-loaded polylactide/poly(butylene adipate-co-terephthalate) blends: nanoparticles' influence on the structure and properties of nanofibrous webs, *Cellulose*, 32(3), 1607–1626.

[13]. Oladele, I. O., Taiwo, A. S. ,Bello, L. J., Balogun, S. O., Sipho, L. S. and Adelani, S. O., (2024). Fabrication of animal shell and sugarcane bagasse particulate hybrid reinforced epoxy composites for structural applications, *Polymer and Polymer Composites*, 32, 1–12.

[14]. Patil, H., Sudagar, I. P., Pandiselvam, R., Sudha, P. and Boomiraj, K., (2023). Development and characterization of rigid packaging material using cellulose/sugarcane bagasse and natural resins, *International Journal of Biological Macromolecules*, 246, 125641.

[15]. Anggono, J. Ágnes E. F. András, B. János, M. Antoni, H. P. and Béla, P., (2019). Deformation and failure of sugarcane bagasse reinforced PP, *European Polymer Journal.*, 112, 153–160.

[16]. Vidyashri, V., Henrita, L., Narayanasamy, P., Mahesha, G. T. and Subrahmanya B. K., 2019. Preparation of Chemically Treated Sugarcane Bagasse Fiber Reinforced Epoxy Composites and Their Characterization *Cogent Engineering*, 6, 1.

[17]. Prasad, L., Kumar, S., Patel, R. V., Yadav, A., Virendra, K. and Winczek, J., (2020). Physical and Mechanical Behaviour of Sugarcane Bagasse Fibre-Reinforced Epoxy Bio-Composites, *Materials (Basel)*, 13, 1– 5387.

[18]. Peng, Y., Lei, W. and Yu, W., (2025). Effect of Sugarcane Bagasse Content and Modification on the Properties of Sugarcane Bagasse / Poly ( lactic Acid ) Biocomposites, *Molecules*, 30, 1-1583.

[19]. Muthu, R. K., Anand, T., Vidyalakshmi, R. and Anandakumar, S., (2019). Fabrication and Property Evaluation of Biodegradable Tableware ( Plate ) Made from Mango Seed Shell, *Indian Journal of Pure and Applied Biosciences*, 1019, 7(1), 448–454.

[20]. Afolalu, S. A., Ogedengbe, T. S., Atotuoma, J. O. and Ikumapayi, O. M., (2024). Development of Biodegradable Food Package Using Agro-Wastes *Journal of Composite and Advanced Materials*, 34(5), 661–666.

[21]. Asrofi, M. Muhammad, O. P. H., Al Anshori, M. L., Putra, F. H., Pradiza, R. R., Setyawan, H., Yusuf, M., Siswanto, M., Ilyas, R. A., Muhammad Rizal, M. A., Sapuan, S. M., Knight, V. F. and Faiz Norrrahim, M. N., (2025). The Effect of Alkalization Fiber on Mechanical , Microstructure , and Thermal Properties of Sugarcane Bagasse Fiber Reinforced PLA Biocomposite, *Journal of Renewable Materials*, 13,10, 1–1979.